AD_____

Award Number: W81XWH-06-1-0352

TITLE: Maintenance of Genome Stability and Breast Cancer: Molecular Analysis of DNA Damage-Activated Kinases

PRINCIPAL INVESTIGATOR: Heather L. Ball
Mark Ehrhardt
Daniel Mordes
David Cortez

CONTRACTING ORGANIZATION: Vanderbilt University Medical Center
Nashville, TN 37232

REPORT DATE: March 2007

TYPE OF REPORT: Annual Summary

PREPARED FOR: U.S. Army Medical Research and Materiel Command
Fort Detrick, Maryland 21702-5012

# REPORT DOCUMENTATION PAGE

*Form Approved*
*OMB No. 0704-0188*



| 1. REPORT DATE | 2. REPORT TYPE | 3. DATES COVERED |
|---|---|---|
| 01-03-2007 | Annual Summary | 15 Feb 2006 – 14 Feb 2007 |

**4. TITLE AND SUBTITLE**

Maintenance of Genome Stability and Breast Cancer: Molecular Analysis of DNA Damage-Activated Kinases

**5a. CONTRACT NUMBER**

**5b. GRANT NUMBER**
W81XWH-06-1-0352

**5c. PROGRAM ELEMENT NUMBER**

**6. AUTHOR(S)**

Heather L. Ball, Mark Ehrhardt, Daniel Mordes, David Cortez

Email: heather.l.ball@vanderbilt.edu

**5d. PROJECT NUMBER**

**5e. TASK NUMBER**

**5f. WORK UNIT NUMBER**

**7. PERFORMING ORGANIZATION NAME(S) AND ADDRESS(ES)**

Vanderbilt University Medical Center
Nashville, TN 37232

**8. PERFORMING ORGANIZATION REPORT NUMBER**

**9. SPONSORING / MONITORING AGENCY NAME(S) AND ADDRESS(ES)**
U.S. Army Medical Research and Materiel Command
Fort Detrick, Maryland 21702-5012

**10. SPONSOR/MONITOR'S ACRONYM(S)**

**11. SPONSOR/MONITOR'S REPORT NUMBER(S)**

**12. DISTRIBUTION / AVAILABILITY STATEMENT**
Approved for Public Release; Distribution Unlimited

**13. SUPPLEMENTARY NOTES**
Original contains colored plates: ALL DTIC reproductions will be in black and white.

**14. ABSTRACT** The ATR (ATM and Rad3-Related) kinase is essential to maintain genomic integrity. ATR is recruited to DNA lesions in part through its association with ATR-interacting protein (ATRIP), which in turn interacts with the single-stranded DNA binding protein RPA (Replication Protein A). In this study, a conserved checkpoint protein recruitment domain (CRD) in ATRIP orthologs has been identified by biochemical mapping of the RPA binding site in combination with NMR, mutagenesis and computational modeling. Mutations in the CRD of the yeast ATRIP ortholog Ddc2 disrupt the Ddc2-RPA interaction, prevent proper localization of Ddc2 to DNA breaks, sensitize yeast to DNA damaging agents, and partially compromise checkpoint signaling. These data demonstrate that the CRD is critical for localization and optimal DNA damage responses. However, the stimulation of ATR kinase activity by binding of TopBP1 to ATRIP-ATR can occur independently of the interaction of ATRIP with RPA. Our results support a multi-step model for ATR activation that requires separable localization and activation functions of ATRIP.

**15. SUBJECT TERMS**
ATR, ATRIP, DNA damage checkpoint, RPA, Ddc2, Mec1.

| 16. SECURITY CLASSIFICATION OF: | | | 17. LIMITATION OF ABSTRACT | 18. NUMBER OF PAGES | 19a. NAME OF RESPONSIBLE PERSON |
|---|---|---|---|---|---|
| a. REPORT | b. ABSTRACT | c. THIS PAGE | | | USAMRMC |
| U | U | U | UU | 50 | 19b. TELEPHONE NUMBER *(include area code)* |

**Table of Contents**

**Page**

**Introduction…….……. 2**

**Body…… 3**

**Key Research Accomplishments…….……. 4**

**Reportable Outcomes…… 4**

**Conclusion…….. 4**

**References…….. 6**

**Appendices……. 7**

**Introduction:**

DNA damage checkpoint responses are key regulators of genomic stability and defects in these signaling pathways promote the transformation of normal cells into cancer cells (15). DNA damage checkpoints have evolved to allow organisms to respond to both endogenous and exogenous DNA damage by inducing a cell cycle arrest to allow the cell time to repair the damage before cell cycle progression is resumed. ATM (Ataxia Telangiectasia Mutated) and ATR (ATM and Rad3-related) are the primary DNA damage checkpoint kinases activated in response to genotoxic lesions including ionizing radiation (IR), ultraviolet radiation (UV) or stalled replication forks (1, 17). Heterozygous mutations in ATM predispose women to breast cancer and are found in approximately 1% of North American women (9, 11, 16). ATR mutations have yet to be linked to breast cancer, but ATR regulates several proteins linked to breast cancer including BRCA1 (breast and ovarian cancer susceptibility) and p53 (8, 10, 15) . The mechanism of ATR activation is unknown and most extensive work has focused on ATR-dependent signaling to substrates (17). As discovered by our laboratory, ATR exists in a stable complex with an associated protein ATRIP (ATR Interacting Protein). ATR and ATRIP are highly conserved and mutations in the yeast ATRIP homologs Rad26 and Ddc2 yield almost identical phenotypes to mutations in ATR homologs Mec1 and Rad3 (14). Based on these data, ATRIP is hypothesized to be a regulator of ATR (7). However, the functional roles of ATRIP and the yeast homologs Rad26 and Ddc2 remain unclear. Our current studies focus on the role of ATRIP in recruiting ATR to sites of DNA damage through a direct interaction between ATRIP and replication protein A (RPA).

**Body:**

ATR-ATRIP is located diffusely throughout the nucleus in undamaged cells. Following exposure of cells to DNA damage, ATR-ATRIP relocalizes to accumulate into distinct nuclear foci that co-localization with other checkpoint and repair proteins as well as phosphorylated γ-H2AX, a marker for DNA damage (13, 14). ATR-ATRIP relocalization to foci requires an interaction between ATRIP and RPA-ssDNA (3). Increasing amounts of RPA-ssDNA are generated during S-phase when a replication fork encounters a DNA lesion and becomes uncoupled. The DNA helicase is not hindered by the lesion and continues to unwind DNA template, whereas the DNA polymerase becomes stalled at the site of the lesion, allowing RPA-ssDNA to be generated (5). For this reason, RPA-ssDNA is thought to be a trigger for ATR activation (5, 6). We identified an N-terminal ATRIP domain required for binding RPA-ssDNA. Deletion of this N-terminal RPA binding domain prevented the accumulation of ATR-ATRIP into nuclear foci, but, surprisingly had no effect on ATR-dependent phosphoarylation of its downstream substrate Chk1 (3). These results suggested that stable retention of ATR at a damage site is not required for ATR activation in response to UV, HU and IR (3).

We have furthered this work through our completion of Task 1 from the statement of work which was to examine the role of ATR localization to sites of DNA damage in ATR activation. Using a combination of biochemical mapping, NMR, mutagenesis and computational modeling we have identified a conserved checkpoint protein recruitment domain (CRD) in ATRIP orthologs. Mutations in the CRD of the yeast ATRIP ortholog Ddc2 disrupt the Ddc2-RPA interaction, prevent proper localization of Ddc2 to DNA

breaks, sensitize yeast to DNA damaging agents, and partially compromise checkpoint signaling (2). These data demonstrate that the CRD is critical for localization and optimal DNA damage responses. Recently, Kumagai et al discovered that a fragment of TopBP1 could activate ATR both in vitro and in vivo. This TopBP1-dependent activation of ATR is ATRIP-dependent, but does not require the ATRIP CRD (2, 12), suggesting that ATRIP contains separate domains involved in RPA-binding dependent recruitment of ATR-ATRIP to DNA lesions and TopBP1-dependent activation of the ATR kinase. Our results, in combination with others, support a multi-step model for ATR activation that requires separable localization and activation functions of ATRIP.

**Key Accomplishments:**

- Publication of manuscript "Function of a conserved checkpoint recruitment domain in ATRIP proteins" in Mol Cell Biol, March 7, 2007.

**Reportable Outcomes:**

- Publication of manuscript "Function of a conserved checkpoint recruitment domain in ATRIP proteins" in Mol Cell Biol, March 7, 2007.
- Presentation of work at International Ataxia Telengiectasia Workshop, September 2006, entitled "Role of a Conserved RPA-ATRIP Interaction in ATR Signaling".
- PhD degree to be obtained August, 2007 for this and previous work.
- Post-doctoral research position secured at Hospital for Sick Kids, University of Toronto, Toronto, Ontario.

**Conclusions:**

ATR kinase activity does not detectably increase following exposure to DNA damage, therefore, the prevailing model for ATR activation was that ATR is constitutively activated and is regulated by subnuclear relocalization to sites of DNA damage where it can access substrates (4). However, mounting evidence, including that supported by this grant, suggest that this model is oversimplified. For example, ATRIP mutants lacking the N-terminal RPA binding domain were unable to accumulate into nuclear foci, however, these localization-defective mutants are able to support the activation of checkpoint signaling, suggesting that foci formation is not required for ATR activation. These data indicate that localization and activation are two separate events in ATR-dependent checkpoint signaling. The recent finding by Kumagai et al that ATR can be activated by TopBP1 helped to fill in some of the missing pieces to the puzzle of how ATR is activated. TopBP1-dependent ATR activation is dependent on ATRIP but not on the RPA-binding domain of ATRIP, suggesting that TopBP1-dependent ATR activation is separate from RPA-dependent ATR-ATRIP recruitment (2, 12). These findings lead to a revised, two-step model of ATR activation and have helped to change the premise in the field as to how ATR checkpoint signaling is activated (12).

ATR, ATM and other checkpoint signaling pathways are activated by many cancer therapies and regulate the cellular outcomes of these treatments. Disruption of ATR, ATM, and DNA-PK kinases sensitizes cells to radiation and chemotherapy. Since mutations in DNA repair and DNA-damage response pathways are common in cancer cells, these cells are particularly sensitive to disruption of additional pathways. This rationale has driven the development of small molecule inhibitors of DNA damage-responsive kinases for use as chemo- or radio-sensitizing agents (22, 32). Thus far,

specific inhibitors of ATM and DNA-PK kinases have been developed, built around competitive inhibition by binding of ATP analogues (19). However, specific inhibitors of the ATR kinase have not been found. Unique properties of ATR such as its requirement for ATRIP may provide an alternative means of disrupting ATR signaling. Hence, in addition to shaping the emerging model of ATR activation, the finding supported by this funding have also furthered our knowledge of the molecular details of a potential target for chemotherapeutics. The molecular characterization of ATRIP structure and function as described here may provide a useful starting point for the development of an ATR targeted therapy.

**References:**


1. **Abraham, R. T.** 2001. Cell cycle checkpoint signaling through the ATM and ATR kinases. Genes Dev **15:**2177-2196.
2. **Ball, H. L., Ehrhardt, M., Mordes, D., Chazin, W., Cortez, D.** 2007. Function of a conserved checkpoint recruitment domain in ATRIP proteins. Mol Cell Biol.
3. **Ball, H. L., J. S. Myers, and D. Cortez.** 2005. ATRIP Binding to RPA-ssDNA Promotes ATR-ATRIP Localization but Is Dispensable for Chk1 Phosphorylation. Mol Biol Cell **16:**2372-2381.
4. **Bartek, J., and N. Mailand.** 2006. TOPping up ATR activity. Cell **124:**888-890.
5. **Byun, T. S., M. Pacek, M. C. Yee, J. C. Walter, and K. A. Cimprich.** 2005. Functional uncoupling of MCM helicase and DNA polymerase activities activates the ATR-dependent checkpoint. Genes Dev.
6. **Cortez, D.** 2005. Unwind and slow down: checkpoint activation by helicase and polymerase uncoupling. Genes Dev **19**.
7. **Cortez, D., S. Guntuku, J. Qin, and S. J. Elledge.** 2001. ATR and ATRIP: partners in checkpoint signaling. Science **294:**1713-1716.
8. **Cortez, D., Y. Wang, J. Qin, and S. J. Elledge.** 1999. Requirement of ATM-dependent phosphorylation of brca1 in the DNA damage response to double-strand breaks. Science **286:**1162-1166.
9. **Ding, S. L., L. F. Sheu, J. C. Yu, T. L. Yang, B. F. Chen, F. J. Leu, and C. Y. Shen.** 2004. Abnormality of the DNA double-strand-break checkpoint/repair genes, ATM, BRCA1 and TP53, in breast cancer is related to tumour grade. Br J Cancer **90:**1995-2001.
10. **Foray, N., D. Marot, A. Gabriel, V. Randrianarison, A. M. Carr, M. Perricaudet, A. Ashworth, and P. Jeggo.** 2003. A subset of ATM- and ATR-

dependent phosphorylation events requires the BRCA1 protein. Embo J **22:**2860-2871.

11. **Khanna, K. K., and G. Chenevix-Trench.** 2004. ATM and genome maintenance: defining its role in breast cancer susceptibility. J Mammary Gland Biol Neoplasia **9:**247-262.
12. **Kumagai, A., J. Lee, H. Y. Yoo, and W. G. Dunphy.** 2006. TopBP1 activates the ATR-ATRIP complex. Cell **124:**943-955.
13. **Lisby, M., J. H. Barlow, R. C. Burgess, and R. Rothstein.** 2004. Choreography of the DNA damage response: spatiotemporal relationships among checkpoint and repair proteins. Cell **118:**699-713.
14. **Melo, J. A., J. Cohen, and D. P. Toczyski.** 2001. Two checkpoint complexes are independently recruited to sites of DNA damage in vivo. Genes Dev **15:**2809-2821.
15. **Motoyama, N., and K. Naka.** 2004. DNA damage tumor suppressor genes and genomic instability. Curr Opin Genet Dev **14:**11-16.
16. **Umesako, S., K. Fujisawa, S. Iiga, N. Mori, M. Takahashi, D. P. Hong, C. W. Song, S. Haga, S. Imai, O. Niwa, and M. Okumoto.** 2005. Atm heterozygous deficiency enhances development of mammary carcinomas in p53 heterozygous knockout mice. Breast Cancer Res **7:**R164-170.
17. **Zhou, B. B., and S. J. Elledge.** 2000. The DNA damage response: putting checkpoints in perspective. Nature **408:**433-439.

**Appendices:**

1. Attached manuscript "Function of a conserved checkpoint recruitment domain in ATRIP proteins."

MCB Accepts, published online ahead of print on 5 March 2007
Mol. Cell. Biol. doi:10.1128/MCB.02238-06


# Function of a Conserved Checkpoint Recruitment Domain in ATRIP Proteins

Heather L. Ball[1], Mark R. Ehrhardt[2], Daniel A. Mordes[1], Gloria G. Glick[1], Walter J. Chazin[2], and David Cortez[1]*

[1]Department of Biochemistry, [2]Departments of Biochemistry and Chemistry and Center for Structural Biology, Vanderbilt University, Nashville TN 37232

*Correspondence should be addressed to:

David Cortez, Ph.D.
Department of Biochemistry
Vanderbilt University
613 Light Hall
23rd @ Pierce Ave.
Nashville, TN 37232
Phone: 615-322-8547
Fax: 615-343-0704
Email: david.cortez@vanderbilt.edu

Running title: FUNCTIONS OF RPA AND TOPBP1 IN ATR-ATRIP SIGNALING

**The ATR (ATM and Rad3-Related) kinase is essential to maintain genomic integrity. ATR is recruited to DNA lesions in part through its association with ATR-interacting protein (ATRIP), which in turn interacts with the single-stranded DNA binding protein RPA (Replication Protein A). In this study, a conserved checkpoint protein recruitment domain (CRD) in ATRIP orthologs has been identified by biochemical mapping of the RPA binding site in combination with NMR, mutagenesis and computational modeling. Mutations in the CRD of the yeast ATRIP ortholog Ddc2 disrupt the Ddc2-RPA interaction, prevent proper localization of Ddc2 to DNA breaks, sensitize yeast to DNA damaging agents, and partially compromise checkpoint signaling. These data demonstrate that the CRD is critical for localization and optimal DNA damage responses. However, the stimulation of ATR kinase activity by binding of TopBP1 to ATRIP-ATR can occur independently of the interaction of ATRIP with RPA. Our results support a multi-step model for ATR activation that requires separable localization and activation functions of ATRIP.**



Keywords: ATR/ ATRIP/ checkpoint/ Ddc2/ RPA

ATR is a protein kinase that coordinates cellular responses to genotoxic stress. ATR activation occurs primarily in S-phase due to replication stress induced by DNA damaging agents or replication inhibitors. More specifically, ATR activation is stimulated when the replication machinery encounters a DNA lesion and becomes uncoupled (the helicase continues to unwind DNA while the polymerase becomes stalled at the site of DNA damage) (9).

The critical factor that promotes ATR activation is believed to be the accumulation of RPA-coated single stranded (ss) DNA (11, 33, 43). At least two separate checkpoint complexes accumulate in distinct foci that co-localize with RPA. Rad17, a PCNA-like clamp loader protein, is recruited to RPA-ssDNA and loads the Rad9-Rad1-Hus1 checkpoint clamp at the junction of double-stranded and single-stranded DNA (4, 14, 53). Independently, ATR is recruited by ATRIP, which binds the RPA-ssDNA that accumulates at DNA lesions (3, 15, 37, 52).

ATRIP is required for ATR function and mutation of either ATR or ATRIP causes identical phenotypes (3, 12). The strict requirement for ATRIP is conserved in *S. pombe* (Rad3 and Rad26), *S. cerevisiae* (Mec1 and Ddc2/Lcd1/Pie1) and *X. laevis* (xATR and xATRIP) (13, 38, 41, 51). An N-terminal domain of ATRIP binds RPA-ssDNA and is necessary for stable ATR-ATRIP localization to damage-induced nuclear foci (3, 25).

The ATR signaling pathway is currently viewed as an important target for the development of cancer therapies (10, 22, 24, 32, 34). However, the mechanism by which ATR is activated remains unclear. Localization to sites of DNA damage or replication stress has been suggested to be essential and perhaps sufficient to promote ATR

signaling. However, mutations in ATRIP that disrupt the stable RPA-ATRIP interaction and impair the accumulation of ATR-ATRIP complexes in DNA-damage induced foci have minimal effects on ATR activation and signaling (3, 25). Furthermore, Topoisomerase Binding Protein 1 (TopBP1) was recently discovered to stimulate ATR kinase activity, suggesting regulation by a means other than localization (28). To clarify the functions of ATRIP, RPA, and TopBP1 in mediating ATR-dependent checkpoint response we have performed a series of biochemical and genetic experiments in human and yeast systems. We report structural and functional data that support a model for ATR activation in which two separable ATRIP activities—localization and activation—cooperate to promote ATR signaling.

## MATERIALS AND METHODS

### Yeast Strains

All strains used in this study are described in Table 1. *Myc-Ddc2* and *Myc-Ddc2* mutant strains were generated by expressing mutants from a centromeric plasmid under the control of the endogenous *DDC2* promoter in strain DMP2995/1B (*Mata sml1D::KanMX4 ddc2D::KanMX4*) (38). *GFP-Ddc2ΔN* was generated in JK8-1 (36) using the delitto perfetto system (47). Strain yHB244 was generated by expressing RNR3 using pBAD79 and deleting *DDC2* using pGEM499 in the JKM179 strain (30). *Myc-DDC2* and *Myc-Ddc2ΔN* were expressed in strain yHB244 from the pNML1 centromeric plasmid (42).

### RPA-ssDNA and RPA Binding

The 14 kDa and 70kDa RPA subunits were tagged with a $His_6$ epitope tag (46). RPA was purified from *E. coli* using nickel affinity chromatography followed by Superdex fractionation. 20 pmol of biotin-labeled 69 base pair single-stranded oligonucleotide was bound to streptavidin beads and incubated either with binding buffer (10mM Tris pH=7.5, 100mM NaCl, 10% glycerol, 0.02% Igepal CA-630, 10µg/ml BSA) alone or a 4 molar excess of RPA in binding buffer. The RPA-ssDNA-streptavidin beads were washed three times with binding buffer prior to use. HA-ATRIP fragments were generated using in vitro transcription/translation (Promega), added to recombinant His-RPA or His-RPA-ssDNA beads in binding buffer and RPA was isolated using His-Select (Sigma Aldrich) or ssDNA-sepharose beads. Proteins bound to beads were washed with binding buffer three times, eluted and separated by SDS-PAGE prior to blotting.

**Kinase assays**

ATR kinase assays were performed essentially as described with the following alterations (28). HA-ATRIP and Flag-ATR expression vectors were transfected into 293T cells and the ATR-ATRIP complexes purified by immunoprecipitation. Kinase reactions were performed with the antibody-linked ATR-ATRIP complex. Recombinant TopBP1 and RPA heterotrimer was purified from *E. coli*. The Phas1 substrate was purchased from A.G. Scientific. The in situ Rad53 autophosphorylation assay following denaturation/renaturation was performed as previously described (39).

**Cell culture**

All cells were grown in DMEM + 7.5% FBS. Plasmid transfections were performed with Lipofectamine 2000 (Invitrogen). The ATRIP wild-type and ATRIPΔN 293T cells were generated by retroviral infection and selection (3). ATRIP siRNA transfections and immunofluorescence methods were also as described (3).

**Protein Purification and Antibodies**

TAP-Rfa1 was purified from soluble yeast extracts as described (1, 17). RPA70N was kindly provided by Cheryl Arrowsmith in a pET15b vector (Novagen), was grown on defined M9 media supplemented with $^{15}$N-ammonium chloride and D-glucose and purified over Ni-NTA. The γH2AX (Upstate), Myc9E10 (Covance), HA.11 (Covance) were purchased from indicated companies. Rad53 antibody was a gift from Dr. Stephen Elledge. Rfa1 antibody was a gift from Dr. Steven Brill.

**NMR Analysis and Homology Modeling**

NMR spectra were collected on ~100 μM $^{15}$N-RPA70N in a buffer containing 2 mM BME, 50 mM NaCl, and 20 mM Tris-$d_{11}$ at pH 7.4. ATRIP1-107 and ATRIP54-70 were added at a 4–6 fold molar excess to maximize the bound state population of the observed component, RPA70N. NMR experiments were performed at 25 ºC using Bruker AVANCE 500 MHz or 600 MHz NMR spectrometers equipped with a 5 mm single axis z-gradient Cryoprobe. Two-dimensional, gradient-enhanced $^{15}$N-$^{1}$H HSQC spectra were recorded with 1024 complex data points in the $^{1}$H and 96 complex points in $^{15}$N dimension. $^{1}$H and $^{15}$N backbone NMR assignments for RPA70N were kindly provided by Dr. Cheryl Arrowsmith.

**Chromatin Immunoprecipitation Analysis**

HO-expression in strains yHB245 (vector), yHB246 (Myc-DDC2) and yHB247 (Myc-Ddc2ΔN) containing galactose-inducible expression of HO endonuclease was as described (30). Cells were crosslinked with 1% formaldehyde, lysed and sonicated to generate DNA with an average size of 500 bp. Myc-Ddc2 protein-DNA complexes were isolated using Myc9E10 antibody and protein G-sepharose beads, washed extensively and eluted from beads. Crosslinks were reversed by incubating overnight at 65°C. DNA was precipitated and amplified using primers specific to a region adjacent to the HO break site (HO-A or HO-B) or to a region of SMC2. HO-A1: 5'CTCATCTGTGATTTGTGG 3', HO-A2: 5'AGAGGGTCACAGCACTAATACA 3', HO-B1: 3'CCAGATTTGTATTAGACGAGGGACGGAGTGA 5', HO-B2:

3’AGAGGGTCACAGCACTAAATACAGCTCGAAT 5’, SMC2-1: 3’ AAGAGAAACTTTAGTCAAAACATGGG 5’, SMC2-2: 3’CCATCACATTATACTAACTACGG 5’.

## RESULTS

### Characterization of ATRIP and RPA Binding Domains

Our analysis started with an examination of the binding of ATRIP fragments to RPA in the absence and presence of ssDNA. Previous analysis of ATRIP identified at least three domains: an N-terminal RPA-ssDNA binding domain, a dimerization domain predicted to fold into a coiled-coil structure, and a C-terminal ATR-interaction domain (2, 3). HA-tagged, intact ATRIP and ATRIP fragments spanning the various domains were generated using a coupled transcription/translation system. These ATRIP proteins were added to purified His-tagged RPA heterotrimer bound to ssDNA displayed on sepharose beads or His-tagged RPA hetrotrimer bound to nickel beads. After incubation and washing, the bound ATRIP proteins were detected by western blot analysis. We found that all ATRIP fragments containing the N-terminal 107 amino acids bound well to RPA-ssDNA and His-RPA in the absence of DNA (Figure 1A and B). Thus, the first 107 amino acids of ATRIP contain a protein-protein interaction domain that mediates binding to the RPA heterotrimer.

HA-ATRIP fragments lacking this N-terminal RPA binding domain of ATRIP (N-RBD) were deficient in binding RPA-ssDNA and His-RPA (Figure 1A and B). Long exposures of western blots did show a small degree of association of these ATRIP fragments with RPA. In fact, all of the protein fragments that we tested including a fragment of Brca1 bound weakly to RPA-ssDNA (Figure 1A). These interactions may reflect additional RPA-ssDNA binding domains on ATRIP as has been previously reported (37).

To determine which subunit of the RPA heterotrimer interacts with ATRIP, we purified recombinant RPA domains individually or in combination as His-tagged proteins (Figure 1C). Using pull-down assays with *in vitro* translated ATRIP proteins, we found that full length HA-ATRIP or the isolated N-RBD only bound to RPA fragments containing the N-terminal RPA70 oligonucleotide/oligosaccharide (OB)-fold domain (RPA70N) (Figure 1D). No significant binding was detectable to other RPA domains and no binding of ATRIPΔN (ATRIP108-791) protein lacking the N-RBD was detectable to any RPA fragment (Figure 1D) in this assay. Taken together, these data suggest that the ATRIP N-RBD interacts directly with the 70N domain of RPA.

**A conserved acidic domain in the ATRIP N-terminus interacts with the basic cleft of the RPA70N OB fold**

The specific residues involved in the interaction of RPA and ATRIP were identified using an NMR chemical shift mapping approach. This strategy involves monitoring NMR chemical shifts of one protein over the course of a titration with a binding partner. Measurement of the RPA $^{15}$N-$^{1}$H-HSQC NMR spectrum of $^{15}$N-enriched RPA70N as ATRIP N-RBD is titrated in solution shows only a subset of the RPA70N signals are affected (Figure 2A). The observation of effects in the fast to intermediate exchange regime on the NMR timescale suggests that binding is occurring with a dissociation constant in the low micromolar range. When the chemical shifts are mapped onto the crystal structure of RPA70N (7), it is apparent that ATRIP N-RBD interacts within the basic cleft of RPA70N (Figure 2B).

Initial insight into the RPA70N binding site of the ATRIP N-RBD was obtained from sequence analysis. When the N-termini of five ATRIP orthologs were aligned, minimal sequence similarity was observed with the notable exception of a small, acidic region spanning approximately fifteen amino acids (Figure 2C). On the basis of putative electrostatic complementarity, we hypothesized that this small acidic region made contact with the basic surface in the cleft of the OB-fold of RPA70N. To test this hypothesis, an ATRIP peptide spanning the conserved acidic region (ATRIP54-70) was synthesized and the RPA70N titration was repeated. The titration with the peptide perturbed most of the same residues as the titration with ATRIP N-RBD indicating that the ATRIP peptide binds in the same manner within the basic cleft of RPA70N (Figure 2D). In addition, we analyzed the binding of ATRIP 1-107 containing charge reversal mutations at positions D58 and D59 to RPA70N using NMR. This mutant binds much more weakly than wild type ATRIP.

The basic cleft of RPA70N has been shown to bind peptides that can mimic DNA in a manner similar to the binding of ssDNA to the A and B domains of RPA70 (5, 7). RPA70N binds an acidic helical peptide of p53, and the crystal structure of the p53 peptide bound in the cleft was determined (7). Alignment of this p53 peptide with ATRIP54-70 indicates significant homology between the two peptides (Figure 2E). Therefore, the crystal structure of RPA70N bound to the p53 peptide was used to generate a homology model for the ATRIP peptide-RPA70N interaction. The strategy involved using the backbone coordinates of the RPA70N and the p53 peptide along with the side-chains of RPA70N from the crystal structure. The p53 amino acid side chains were replaced with the ATRIP amino acid 55-66 side chains, and the best fit of the

ATRIP peptide into the constrained RPA70N was determined using ROSETTA (Figure 2F) (40).

The model predicts that there are several specific electrostatic interactions between the acidic residues on ATRIP and the basic residues on RPA. In particular, the absolutely conserved aspartic acid residues D58 and D59 of ATRIP are likely to make contacts with R41 and K88 of RPA70N (Figure 2G). Basic residues at these positions in RPA are highly conserved. The NMR data and molecular modeling are fully consistent with the previously described pull-down experiments, indicating that the N-terminus of ATRIP binds directly to RPA70N. Importantly, these data create a structural framework within which specific ATRIP-RPA binding mutants can be designed and used for functional analysis.

**The N-RBD of human ATRIP is conserved in the *S. cerevisiae* ATRIP ortholog Ddc2**

The functional consequences of disrupting the ATRIP-RPA interaction in human cells was previously characterized using an ATRIP mutant lacking the entire N-RBD (ATRIPΔN). Unlike wild-type ATRIP, ATRIPΔN has a severe defect in localizing to damage- or replication stress-induced nuclear foci (3). Despite this localization defect, cells depleted of endogenous ATRIP and complemented with ATRIPΔN have normal ATR-dependent signaling following DNA damage (3). The only checkpoint defect that we have uncovered in the ATRIPΔN expressing cells is a slight delay in recovering from hydroxyurea (HU)-induced stalling of replication (H.B. unpublished data). RNA interference of endogenous ATRIP synthesis is not 100% effective and is variable from cell to cell. In addition, the level of retrovirally expressed ATRIP or ATRIPΔN after

integration of the retroviral vector is variable and not equivalent to the endogenous protein levels (3). These technical limitations to performing genetics in human cell culture may confound our ability to detect the phenotypic consequences of abrogating the ATRIP-RPA interaction. Therefore, we sought to examine the physiological role of the ATRIP-RPA interaction in another genetic system - *S. cerevisiae*.

The RPA binding domain of ATRIP is N-terminal to the predicted coiled-coil domain. To determine if the equivalent region of yeast ATRIP (Ddc2) mediates binding to yeast RPA70 (Rfa1), we deleted 42 amino acids N-terminal to the predicted coiled-coil domain of Ddc2 (Ddc2ΔN) (Figure 3A). Binding of Ddc2 and Ddc2ΔN to Rfa1 was assayed using co-immunoprecipitation. Myc-tagged Ddc2 (WT) or Ddc2ΔN (ΔN) were expressed from plasmids under control of the endogenous *DDC2* promoter in Δ*ddc2* cells containing HA-tagged Mec1. Myc-Ddc2 and Myc-Ddc2ΔN were immunoprecipitated using a Myc antibody and co-associated Rfa1 and Mec1 were assayed by western blotting. As expected, both Mec1 and Rfa1 were co-immunoprecipitated with Ddc2 (Figure 3B). In comparison, Rfa1 association with Ddc2ΔN was greatly reduced although Ddc2ΔN continued to bind Mec1 (Figure 3B). This data suggests that the N-terminus of Ddc2 is required for a stable Ddc2-Rfa1 interaction. The amount of Rfa1-associated Ddc2 was not altered by exposing cells to UV damage, suggesting that the Ddc2-Rfa1 interaction may not be regulated by DNA damage (Figure 3B). However, these experiments utilize soluble extracts so it is possible that the interaction with DNA-bound RPA is regulated.

Sequence alignment of human and yeast ATRIP indicates that the small acidic region in the ATRIP N-RBD is conserved (Figure 2C). The homology model generated

from NMR data predicts that the absolutely conserved aspartic acid residues in this region (D12 and D13 in Ddc2) could make contacts with conserved basic amino acids on yeast Rfa1. Therefore, we hypothesized that mutating these residues would disrupt Ddc2-Rfa1 binding. To test this hypothesis a Ddc2 mutant was generated with aspartic acid to lysine charge-reversal mutations in these two aspartic acids (Ddc2DK) (Figure 3C). In addition, a mutant (Ddc2N14) was generated replacing Ddc2 residues 14-19 with a peptide (NAAIRS) that is known to adopt a helical conformation (Figure 3C). Myc-Ddc2, Myc-Ddc2ΔN, Myc-Ddc2DK or Myc-Ddc2N14 was expressed in a yeast strain containing TAP-tagged Rfa1. TAP purification of Rfa1 protein complexes indicated they contained Myc-Ddc2 whether or not cells were pre-treated with MMS (Figure 3D). In contrast, TAP-Rfa1 purifications contained minimal Myc-Ddc2ΔN, Myc-Ddc2DK or Myc-Ddc2N14 protein (Figure 3C). These results confirm that the conserved acidic region in the N-terminus of Ddc2 is required for a stable Ddc2-Rfa1 association.

**Ddc2-Rfa1 interaction is required for localization of Ddc2 to sites of DNA damage**

Human ATRIP lacking the N-terminal RPA binding domain (ATRIPΔN) is defective in DNA-damage induced foci formation (3). To determine if the interaction between the N-terminus of Ddc2 and Rfa1 is also required for the localization of Ddc2 to sites of DNA damage we assayed Ddc2 localization using chromatin immunoprecipitation (ChIP) analysis and foci formation. To do this we used the inducible HO nuclease system which introduces a single double-strand break in the yeast genome (29). The induction of a double strand break in Δ*ddc2*, *DDC2* or *ddc2ΔN* yeast strains harboring a galactose-inducible HO endonuclease was diagnosed by comparing PCR products generated using

primer sets adjacent to or spanning the HO cleavage site and was equal in all strains. One hour after HO-induction, cells were treated with crosslinking agent, lysed, sonicated and Myc-Ddc2 protein-DNA complexes were isolated by immunoprecipitation. Myc-Ddc2 bound DNA fragments were recovered and amplified by PCR using two different HO primer sets (HO-A and HO-B) adjacent to the HO cleavage site. As a control we amplified a region of the *SMC2* gene that is on a different chromosome than the HO cleavage site. Wild-type Ddc2 specifically accumulated at the HO cleavage site but not the SMC2 site after induction of the HO endonuclease (Figure 4A). Compared to wild-type Ddc2, the accumulation of Ddc2ΔN at the HO break site was severely reduced although not completely abrogated (Figure 4A). Quantitation of ChIP experiments indicated that Ddc2 binding to the HO-cleavage site is five-fold greater than Ddc2ΔN binding. Ddc2 and Ddc2ΔN were expressed at equal levels and the efficiency of immunoprecipitation was equal in all samples (Figure 4B).

To determine if the defect in Ddc2ΔN accumulation at sites of DNA double strand breaks as detected using ChIP correlated with a defect in accumulation of Ddc2ΔN into DNA-damage induced nuclear foci we fused a C-terminal GFP tag onto Ddc2 and Ddc2ΔN. Equal expression of GFP-Ddc2 and GFP-Ddc2ΔN was assessed by western blotting with an antibody specific to the GFP tag (Figure 4C). HO-endonuclease expression in *GFP-DDC2* and *GFP-ddc2ΔN* strains was induced and Ddc2 localization monitored by fluorescence microscopy. Induction of a DNA break caused GFP-Ddc2 to accumulate into one distinct focus per cell in 40% and 42% of the cells at 4hr and 6hr after HO-induction respectively (Figure 4D and E). Unlike GFP-Ddc2, GFP-Ddc2ΔN formed a focus in only 13% and 19% of cells after 4 hr and 6 hr of HO induction

respectively (Figure 4D and E). Additionally, in cells that did demonstrate HO-induced GFP- Ddc2ΔN foci, the foci were noticeably smaller than GFP-Ddc2 foci (Figure 4D). Taken together, these data demonstrate that, consistent with the role of ATRIP-RPA interaction in human cells, Ddc2-Rfa1 interaction is required for efficient localization of Ddc2 to sites of DNA damage. Since the N-RBD of both ATRIP and Ddc2 is required for recruitment of the ATR-ATRIP/Mec1-Ddc2 checkpoint complexes to DNA lesions, we have named this domain the checkpoint protein recruitment domain (CRD).

**Disruption of the Ddc2-Rfa1 interaction sensitizes cells to DNA damage**

To examine the function of the Ddc2-Rfa1 interaction in Mec1-dependent checkpoint signaling, we first determined if disrupting binding sensitized cells to replication stress or DNA damage. Δ*ddc2* yeast expressing Ddc2, Ddc2ΔN, Ddc2DK or Ddc2N14 were grown to log phase in liquid culture and plated onto media containing increasing amounts of HU or MMS. Yeast lacking Ddc2 altogether are extremely sensitive to even low doses of HU or MMS (Figure 5A and B). In contrast, none of the mutant *ddc2* strains were sensitive to low doses of HU and only a very small difference was visible compared to the *DDC2* strain at the highest HU concentration (Figure 5A). The difference in sensitivity to genotoxic agents between wild type and mutant strains was more apparent in response to the MMS. *ddc2ΔN*, *ddc2DK* and *ddc2N14* strains were more sensitive to high doses of MMS than the *DDC2* strain but much less sensitive than Δ*ddc2* yeast. For example, at a dose of 0.01% MMS, *ddc2ΔN* cell viability was reduced to 3% compared to 23% for *DDC2* and less than 0.01% for Δ*ddc2* yeast (Figure 5B). At 0.15% MMS there was an order of magnitude difference in the viability of *ddc2ΔN ddc2DK* and *ddc2N14*

strains compared to wild-type *DDC2* (Figure 5B). These results suggest that the Ddc2 CRD is important for survival of cells following exposure to the DNA alkylating agent MMS.

To directly examine the role of the Ddc2 CRD in checkpoint signaling, we tested the ability of wild type Ddc2 or Ddc2 mutants to support Mec1-dependent Rad53 phosphorylation. Yeast were grown to log phase, arrested in G1 with alpha factor, released in the presence or absence of 200 mM HU and harvested at various time points after release. Cell lysates were generated and proteins were separated by SDS-PAGE and blotted using antibodies to Rad53. Rad53 phosphorylation is detectable by an electrophoretic mobility shift and is defective in Δ*ddc2* yeast as seen by the absence of a slower migrating form of Rad53 (Figure 5C). Consistent with the lack of HU sensitivity, Ddc2-Rfa binding mutants Ddc2ΔN, Ddc2DK and Ddc2N14 all support Rad53 phosphorylation after exposure to HU as efficiently as Ddc2 (Figure 5C). Detailed time course and dose response experiments also failed to detect a significant Rad53 activation defect in the Rfa1-binding mutant strains in response to HU (Figure 5D and E). These results are consistent with the effects of equivalent mutations in human ATRIP which fail to disrupt ATR signaling in response to HU (3).

In contrast, we did observe an attenuation of Mec1 signaling in these yeast strains in response to MMS. Strains were grown to log phase, arrested in G1 with alpha factor and released into media containing various doses of MMS. Phosphorylated Rad53 is visible in *DDC2* cells after the addition of 0.01% MMS (Figure 5F). However, Rad53 phosphorylation is attenuated in *ddc2ΔN* cells, indicating that optimal Rad53 phosphorylation after exposure to MMS depends upon Ddc2-Rfa1 binding (Figure 5F).

The defect in Mec1 signaling after MMS treatment was most apparent at early time points after release into S-phase (Figure 5G). For example, at the 60-minute time point in the presence of either 0.005% or 0.01% MMS both the phosphorylation dependent-shift of Rad53 and Rad53 kinase activity are significantly reduced in the *ddc2ΔN* strain compared to *DDC2* (Figure 5G). However at later time points (90 min), cells expressing Ddc2ΔN have considerable Rad53 activation whereas Δ*ddc2* cells do not (Figure 5G). These defects at early time points are not due to a difference in the release of yeast from alpha factor arrest since all strains released equivalently. Taken together, these results suggest that Ddc2-Rfa1 binding and localization to damage sites is required for optimal checkpoint activation after exposure to MMS.

**TopBP1-dependent ATR activation can occur independently of RPA**

TopBP1 was recently shown to bind and activate ATR (28). This activation activity was localized to a small fragment of TopBP1 between two BRCT repeat domains. These authors also found that TopBP1 binding and activation of xATR requires xATRIP. We confirmed that TopBP1 activates ATR-ATRIP complexes in an ATRIP-dependent manner (Figure 6 and data not shown). To determine whether the ATRIP CRD influences TopBP1 activation of ATR, we purified either wild type ATR-ATRIP complexes or ATR-ATRIPΔN complexes. Addition of the TopBP1 fragment but not an equivalent fragment containing an inactivating mutation (W1145R) to ATR-ATRIP complexes stimulated ATR activity towards substrates in an immune complex kinase reaction (Figure 6A). Activation of the ATR-ATRIPΔN complex upon the addition of TopBP1 was equal to the activation of ATR-ATRIP (Figure 6A). These findings are consistent

with Kumagai et al who found that xTopBP1 stimulates activation of xATR-xATRIP complexes containing a xATRIP protein lacking the N-terminus (28). Therefore, TopBP1-dependent ATR activation does not require the ATRIP CRD.

We next assayed whether RPA or RPA-ssDNA influences ATR activity or TopBP1-dependent ATR activation. Addition of TopBP1 to ATR-ATRIP stimulated ATR kinase activity (Figure 6B). In contrast, addition of RPA (data not shown) or RPA-ssDNA to ATR kinase assays failed to stimulate ATR activity (Figure 6B). RPA-ssDNA also had no influence on TopBP1-activation of ATR (Figure 6B). RPA32 phosphorylation by ATR is stimulated by TopBP1. In addition, we also observed significant phosphorylation of the TopBP1 fragment, ATRIP, and ATR in these experiments. However, in contrast to the other proteins added to the kinase assay, the amount of autophosphorylation on the ATR-ATRIP complex was not altered significantly by the addition of the TopBP1 fragment. These results suggest that RPA-ssDNA binding to ATR-ATRIP does not influence the kinase activity of ATR. Furthermore, the function of ATRIP required to promote TopBP1-dependent activation of ATR can be separated from its RPA binding activity. However, the results do not exclude the possibility that specific RPA-DNA structures found in cells might regulate kinase activity.

To confirm these results in cells, a GFP-TopBP1 fragment containing the region that activates ATR was transfected into human cells. The cells were engineered to stably express siRNA resistant wild type ATRIP, ATRIPΔN or an empty vector, and were transfected with the ATRIP siRNA prior to GFP-TopBP1 transfection. Depletion of endogenous ATRIP by siRNA transfection in these cells is approximately 80% (3). Twenty-four hours after transfection of the GFP-TopBP1, cells were fixed and stained for

a marker of ATR activation (γH2AX). Overexpression of GFP-TopBP1 in cells containing wild type ATRIP or ATRIPΔN caused phosphorylation of H2AX throughout the chromatin (not in distinct foci as would be observable in response to a DNA damaging agent) (Figure 6C). However, both the intensity of phosphorylation and the number of cells containing phosphorylated H2AX was greatly reduced in cells depleted of ATRIP indicating it is due to ATR-ATRIP signaling (Figure 6C and D). These results confirm that TopBP1 can activate ATR in cells when highly overexpressed even when ATR-ATRIP complexes lack the RPA binding domain and fail to localize to specific sites of DNA damage or replication stress. The overexpression of the TopBP1 fragment likely bypasses the regulation of TopBP1-dependent ATR activation that exists under physiological conditions.



**DISCUSSION**

A checkpoint protein recruitment domain (CRD) has been identified in the N-terminus of ATRIP and Ddc2. This domain binds directly to RPA70N, recruits ATR-ATRIP/Mec1-Ddc2 complexes to sites of DNA damage and promotes ATR-dependent checkpoint signaling in response to MMS. These findings are consistent with Kim et. al. who reported that an N-terminal domain of *Xenopus* ATRIP is required for binding to RPA (25). RPA is a modular protein and it often makes more than one contact with its interacting partners. Indeed, Zou et. al. identified three large regions of ATRIP that may interact with RPA-ssDNA (37). Since no functional data was reported, additional experiments will be required to define and study the function of any other ATRIP

surfaces that make direct contacts with RPA subunits. However, our data indicate that the N-terminal CRD domains of ATRIP and Ddc2 are required for the stable binding of ATRIP/Ddc2 to RPA, and necessary for retention of ATR-ATRIP/Mec1-Ddc2 at sites of DNA damage in cells.

A model of the interaction of RPA70N with a conserved ATRIP peptide within the CRD was generated using NMR data and molecular modeling from the crystal structure of a p53 peptide bound to RPA70N. The model predicts that acidic ATRIP residues (D58 and D59) make direct contacts with basic RPA70N residues (R41 and K88) in the basic cleft of the RPA70N OB fold domain. All of these amino acids are highly conserved. As predicted by this model, mutations reversing the charges on the equivalent aspartic acid residues in Ddc2 (D12K and D13K) abrogate binding to Rfa1. Interestingly, the well characterized *rfa1-t11* mutant, which is known to be replication competent but DNA-damage response deficient, contains a single charge reversal mutation at K45, the equivalent residue to R41 in human RPA (49). Indeed, as our model would predict, rfa-t11 is deficient in recruiting Ddc2 to double strand breaks (23, 52) and in binding Ddc2 (H.B. unpublished data). The *rfa-t11* mutant is also recombination deficient, suggesting that this basic cleft in RPA70N may be a key ligand in DNA damage responses (44, 49). It will be interesting to determine whether other DNA damage response proteins also contain acidic helices that bind within this cleft of RPA70N. It is also noteworthy that an ATR phosphorylation site (S68) is located within the ATRIP CRD just downstream of the acidic peptide that binds to the RPA basic cleft (21). Moreover, RPA70N appears to interact with the RPA32 N-terminus when it is

phosphorylated by checkpoint kinases (6). Therefore, phosphorylation of either ATRIP or RPA may be a means to regulate the ATR-RPA interaction.

The phenotypic consequences of disrupting the ATRIP CRD-RPA70 interaction are similar in both human and yeast cells. In contrast to ATRIP or Ddc2 loss of function, cells containing mutations that disrupt the CRD are only mildly sensitive to DNA damaging agents and partially compromised in checkpoint signaling. In fact, the response to HU is nearly indistinguishable from wild type despite severe defects in ATR-ATRIP/Mec1-Ddc2 localization. Functions of ATRIP in addition to RPA binding are also critical for ATR signaling. These functions include oligomerization (2, 20), ATR stabilization (12) and an undefined activity important for TopBP1-dependent activation of ATR.

The reason for the increased sensitivity of Ddc2 lacking the CRD to damage that generates DNA adducts (MMS) compared to depletion of nucleotides (HU) is unknown. Both types of genotoxic stress activate Mec1 during replication and stall replication forks (48). One potential explanation for this difference may be the amount of RPA-ssDNA present at various types of DNA lesions. Mec1-Ddc2ΔN complexes may have some residual association with Rfa1 and can still partially localize to double strand breaks. Perhaps there is more RPA-ssDNA at an HU-stalled fork than at an MMS-induced lesion, increasing the requirement for the Ddc2 CRD at the MMS lesion. Alternatively the recruitment and activation mechanisms of ATR-ATRIP and Mec1-Ddc2 at MMS or HU lesions may be different. Accumulating evidence suggests that additional protein-protein and protein-DNA interactions other than the ATRIP-RPA interaction may help recruit ATR-ATRIP to DNA lesions (8, 50). Also, Ddc2 contains a DNA end-binding activity

localized to a region C-terminal to the predicted coiled-coil domain (42). Perhaps these alternative modes of ATR-ATRIP/Mec1-Ddc2 recruitment function differently at an HU or MMS lesion.

Consistent with the report by Kumagai and coworkers, we have found that TopBP1 activates ATR, TopBP1-dependent activation of ATR is ATRIP dependent, and it does not require the ATRIP CRD (28). RPA-ssDNA, in contrast, does not stimulate ATR kinase activity in immune complex *in vitro* kinase reactions, and TopBP1-dependent activation of ATR is not altered by adding RPA or RPA-ssDNA to the kinase reaction. These results suggest that TopBP1-dependent ATR activation can be separated from ATRIP-RPA binding. The affinity of TopBP1 for ATR-ATRIP is weak and difficult to detect by co-immunoprecipitations (28). The accumulation of ATR-ATRIP and TopBP1 at sites of damage may facilitate this low-affinity interaction by increasing the local concentration of these proteins.

Taken together, these data support a multi-step model proposed by Dunphy and colleagues (27) for the activation of ATR checkpoint signaling. ATR recruitment to sites of DNA damage and replication stress occurs in part through a direct interaction between the ATRIP CRD and RPA70N. TopBP1 is recruited independently through an interaction with Rad9 (16, 18, 35, 45). The assembly of ATR-ATRIP and TopBP1 at the lesion facilitates TopBP1-dependent ATR activation and in turn, phosphorylation of ATR substrates. Accessory proteins such as claspin are also required for phosphorylation of specific substrates (26, 31). Localization may also serve to bring ATR to the vicinity of key substrates involved in fork stabilization or other aspects of checkpoint regulation. Within this model, ATRIP is a key ATR regulator since it promotes both the localization

and activation of ATR. The model suggests that ATR localization to a damage site precedes its activation. However, it remains possible that ATR can be activated without localization. Indeed, when TopBP1 is highly overexpressed it activates ATR throughout the nucleus in the absence of a DNA lesion (Figure 6C). Furthermore, stable retention of ATR at a damage site is not required for ATR activation at least in response to relatively high doses of UV (3). Thus, further experiments are required to definitively determine whether localization must precede activation.

ATR, ATM and other checkpoint signaling pathways are activated by many cancer therapies and regulate the cellular outcomes of these treatments. Disruption of ATR, ATM, and DNA-PK kinases sensitizes cells to radiation and chemotherapy. Since mutations in DNA repair and DNA-damage response pathways are common in cancer cells, these cells are particularly sensitive to disruption of additional pathways. This rationale has driven the development of small molecule inhibitors of DNA damage-responsive kinases for use as chemo- or radio-sensitizing agents (22, 32). Thus far, specific inhibitors of ATM and DNA-PK kinases have been developed, built around competitive inhibition by binding of ATP analogues (19). However, specific inhibitors of the ATR kinase have not been found. Unique properties of ATR, such as its requirement for ATRIP, may provide an alternative means of disrupting ATR signaling. Hence, the molecular characterization of ATRIP structure and function as described here may provide a useful starting point for the development of an ATR targeted therapy.

**Acknowledgements**

We thank Dr. William Dunphy, Dr. Steve Jackson, Dr. Mike Resnick, Dr. Stephen Elledge, Dr. Steven Brill, Dr. Tony Weil and Dr. Jim Haber for reagents. We thank Dr. Cheryl Arrowsmith for reagents and RPA70N NMR assignments, and Susan M. Meyn, Marie-Eve Chagot and Kristian Kaufmann for assistance in preparation of peptide and protein samples and homology modeling. This work was supported by grants from the National Cancer Institute (R01CA102729 to D.C.) and the National Institute of General Medical Sciences (W.J.C.). D.C. is also supported by the Pew Scholars Program in the Biological Sciences, sponsored by the Pew Charitable Trusts. H.B. is supported by a Department of Defense pre-doctoral fellowship and M.R.E. by an institutional training grant from the National Institute of Environmental Health Sciences. Support for facilities was provided by grants to the Vanderbilt-Ingram Cancer Center (National Cancer Institute) and the Vanderbilt Center in Molecular Toxicology (NIEHS grant P30ES000267).

**References**


1. **Amberg, D. C., Burke, D.J., and Strathern, J.E.** 2005. Methods in Yeast Genetics: A Cold Spring Harbor Laboratory Course Manual.
2. **Ball, H. L., and D. Cortez.** 2005. ATRIP oligomerization is required for ATR-dependent checkpoint signaling. J Biol Chem **280:**31390-31396.
3. **Ball, H. L., J. S. Myers, and D. Cortez.** 2005. ATRIP Binding to RPA-ssDNA Promotes ATR-ATRIP Localization but Is Dispensable for Chk1 Phosphorylation. Mol Biol Cell **16:**2372-2381.
4. **Bermudez, V. P., L. A. Lindsey-Boltz, A. J. Cesare, Y. Maniwa, J. D. Griffith, J. Hurwitz, and A. Sancar.** 2003. Loading of the human 9-1-1 checkpoint complex onto DNA by the checkpoint clamp loader hRad17-replication factor C complex in vitro. Proc Natl Acad Sci U S A **100:**1633-1638.
5. **Binz, S. K., Y. Lao, D. F. Lowry, and M. S. Wold.** 2003. The phosphorylation domain of the 32-kDa subunit of replication protein A (RPA) modulates RPA-DNA interactions. Evidence for an intersubunit interaction. J Biol Chem **278:**35584-35591.
6. **Binz, S. K., A. M. Sheehan, and M. S. Wold.** 2004. Replication Protein A phosphorylation and the cellular response to DNA damage. DNA Repair (Amst) **3:**1015-1024.
7. **Bochkareva, E., L. Kaustov, A. Ayed, G. S. Yi, Y. Lu, A. Pineda-Lucena, J. C. Liao, A. L. Okorokov, J. Milner, C. H. Arrowsmith, and A. Bochkarev.** 2005. Single-stranded DNA mimicry in the p53 transactivation domain interaction with replication protein A. Proc Natl Acad Sci U S A **102:**15412-15417.
8. **Bomgarden, R. D., D. Yean, M. C. Yee, and K. A. Cimprich.** 2004. A novel protein activity mediates DNA binding of an ATR-ATRIP complex. J Biol Chem **279:**13346-13353.
9. **Byun, T. S., M. Pacek, M. C. Yee, J. C. Walter, and K. A. Cimprich.** 2005. Functional uncoupling of MCM helicase and DNA polymerase activities activates the ATR-dependent checkpoint. Genes Dev.
10. **Collins, I., and M. D. Garrett.** 2005. Targeting the cell division cycle in cancer: CDK and cell cycle checkpoint kinase inhibitors. Curr Opin Pharmacol **5:**366-373.
11. **Cortez, D.** 2005. Unwind and slow down: checkpoint activation by helicase and polymerase uncoupling. Genes Dev **19**.
12. **Cortez, D., S. Guntuku, J. Qin, and S. J. Elledge.** 2001. ATR and ATRIP: partners in checkpoint signaling. Science **294:**1713-1716.
13. **Edwards, R. J., N. J. Bentley, and A. M. Carr.** 1999. A Rad3-Rad26 complex responds to DNA damage independently of other checkpoint proteins. Nat Cell Biol **1:**393-398.
14. **Ellison, V., and B. Stillman.** 2003. Biochemical characterization of DNA damage checkpoint complexes: clamp loader and clamp complexes with specificity for 5' recessed DNA. PLoS Biol **1:**E33.
15. **Falck, J., J. Coates, and S. P. Jackson.** 2005. Conserved modes of recruitment of ATM, ATR and DNA-PKcs to sites of DNA damage. Nature **434:**605-611.

16. **Furuya, K., M. Poitelea, L. Guo, T. Caspari, and A. M. Carr.** 2004. Chk1 activation requires Rad9 S/TQ-site phosphorylation to promote association with C-terminal BRCT domains of Rad4TOPBP1. Genes Dev **18:**1154-1164.
17. **Ghaemmaghami, S., W. K. Huh, K. Bower, R. W. Howson, A. Belle, N. Dephoure, E. K. O'Shea, and J. S. Weissman.** 2003. Global analysis of protein expression in yeast. Nature **425:**737-741.
18. **Greer, D. A., B. D. Besley, K. B. Kennedy, and S. Davey.** 2003. hRad9 rapidly binds DNA containing double-strand breaks and is required for damage-dependent topoisomerase II beta binding protein 1 focus formation. Cancer Res **63:**4829-4835.
19. **Hickson, I., Y. Zhao, C. J. Richardson, S. J. Green, N. M. Martin, A. I. Orr, P. M. Reaper, S. P. Jackson, N. J. Curtin, and G. C. Smith.** 2004. Identification and characterization of a novel and specific inhibitor of the ataxia-telangiectasia mutated kinase ATM. Cancer Res **64:**9152-9159.
20. **Itakura, E., I. Sawada, and A. Matsuura.** 2005. Dimerization of the ATRIP Protein through the Coiled-Coil Motif and Its Implication to the Maintenance of Stalled Replication Forks. Mol Biol Cell **16:**5551-5562.
21. **Itakura, E., K. Umeda, E. Sekoguchi, H. Takata, M. Ohsumi, and A. Matsuura.** 2004. ATR-dependent phosphorylation of ATRIP in response to genotoxic stress. Biochem Biophys Res Commun **323:**1197-1202.
22. **Kaelin, W. G., Jr.** 2005. The concept of synthetic lethality in the context of anticancer therapy. Nat Rev Cancer **5:**689-698.
23. **Kanoh, Y., K. Tamai, and K. Shirahige.** 2006. Different requirements for the association of ATR-ATRIP and 9-1-1 to the stalled replication forks. Gene **377C:**88-95.
24. **Kawabe, T.** 2004. G2 checkpoint abrogators as anticancer drugs. Mol Cancer Ther **3:**513-519.
25. **Kim, S. M., A. Kumagai, J. Lee, and W. G. Dunphy.** 2005. Phosphorylation of Chk1 by ATM- and Rad3-related (ATR) in xenopus egg extracts requires binding of ATRIP to ATR but not the stable DNA-binding or coiled-coil domains of ATRIP. J Biol Chem **280:**38355-38364.
26. **Kumagai, A., and W. G. Dunphy.** 2000. Claspin, a novel protein required for the activation of Chk1 during a DNA replication checkpoint response in Xenopus egg extracts. Mol Cell **6:**839-849.
27. **Kumagai, A., and W. G. Dunphy.** 2006. How cells activate ATR. Cell Cycle **5:**1265-1268.
28. **Kumagai, A., J. Lee, H. Y. Yoo, and W. G. Dunphy.** 2006. TopBP1 activates the ATR-ATRIP complex. Cell **124:**943-955.
29. **Lee, S. E., J. K. Moore, A. Holmes, K. Umezu, R. D. Kolodner, and J. E. Haber.** 1998. Saccharomyces Ku70, mre11/rad50 and RPA proteins regulate adaptation to G2/M arrest after DNA damage. Cell **94:**399-409.
30. **Lee, S. E., A. Pellicioli, M. B. Vaze, N. Sugawara, A. Malkova, M. Foiani, and J. E. Haber.** 2003. Yeast Rad52 and Rad51 recombination proteins define a second pathway of DNA damage assessment in response to a single double-strand break. Mol Cell Biol **23:**8913-8923.

31. **Liu, S., S. Bekker-Jensen, N. Mailand, C. Lukas, J. Bartek, and J. Lukas.** 2006. Claspin operates downstream of TopBP1 to direct ATR signaling towards Chk1 activation. Mol Cell Biol **26:**6056-6064.
32. **Lord, C. J., M. D. Garrett, and A. Ashworth.** 2006. Targeting the double-strand DNA break repair pathway as a therapeutic strategy. Clin Cancer Res **12:**4463-4468.
33. **Lukas, J., C. Lukas, and J. Bartek.** 2004. Mammalian cell cycle checkpoints: signalling pathways and their organization in space and time. DNA Repair (Amst) **3:**997-1007.
34. **Luo, Y., and J. D. Leverson.** 2005. New opportunities in chemosensitization and radiosensitization: modulating the DNA-damage response. Expert Rev Anticancer Ther **5:**333-342.
35. **Makiniemi, M., T. Hillukkala, J. Tuusa, K. Reini, M. Vaara, D. Huang, H. Pospiech, I. Majuri, T. Westerling, T. P. Makela, and J. E. Syvaoja.** 2001. BRCT domain-containing protein TopBP1 functions in DNA replication and damage response. J Biol Chem **276:**30399-30406.
36. **Melo, J. A., J. Cohen, and D. P. Toczyski.** 2001. Two checkpoint complexes are independently recruited to sites of DNA damage in vivo. Genes Dev **15:**2809-2821.
37. **Namiki, Y., and L. Zou.** 2006. ATRIP associates with replication protein A-coated ssDNA through multiple interactions. Proc Natl Acad Sci U S A **103:**580-585.
38. **Paciotti, V., M. Clerici, G. Lucchini, and M. P. Longhese.** 2000. The checkpoint protein Ddc2, functionally related to S. pombe Rad26, interacts with Mec1 and is regulated by Mec1-dependent phosphorylation in budding yeast. Genes Dev **14:**2046-2059.
39. **Pellicioli, A., C. Lucca, G. Liberi, F. Marini, M. Lopes, P. Plevani, A. Romano, P. P. Di Fiore, and M. Foiani.** 1999. Activation of Rad53 kinase in response to DNA damage and its effect in modulating phosphorylation of the lagging strand DNA polymerase. Embo J **18:**6561-6572.
40. **Rohl, C. A., C. E. Strauss, D. Chivian, and D. Baker.** 2004. Modeling structurally variable regions in homologous proteins with rosetta. Proteins **55:**656-677.
41. **Rouse, J., and S. P. Jackson.** 2000. LCD1: an essential gene involved in checkpoint control and regulation of the MEC1 signalling pathway in Saccharomyces cerevisiae. Embo J **19:**5801-5812.
42. **Rouse, J., and S. P. Jackson.** 2002. Lcd1p recruits Mec1p to DNA lesions in vitro and in vivo. Mol Cell **9:**857-869.
43. **Shechter, D., V. Costanzo, and J. Gautier.** 2004. Regulation of DNA replication by ATR: signaling in response to DNA intermediates. DNA Repair (Amst) **3:**901-908.
44. **Soustelle, C., M. Vedel, R. Kolodner, and A. Nicolas.** 2002. Replication protein A is required for meiotic recombination in Saccharomyces cerevisiae. Genetics **161:**535-547.

45. **St Onge, R. P., B. D. Besley, J. L. Pelley, and S. Davey.** 2003. A role for the phosphorylation of hRad9 in checkpoint signaling. J Biol Chem **278:**26620-26628.
46. **Stauffer, M. E., and W. J. Chazin.** 2004. Physical interaction between replication protein A and Rad51 promotes exchange on single-stranded DNA. J Biol Chem **279:**25638-25645.
47. **Storici, F., L. K. Lewis, and M. A. Resnick.** 2001. In vivo site-directed mutagenesis using oligonucleotides. Nat Biotechnol **19:**773-776.
48. **Tercero, J. A., M. P. Longhese, and J. F. Diffley.** 2003. A central role for DNA replication forks in checkpoint activation and response. Mol Cell **11:**1323-1336.
49. **Umezu, K., N. Sugawara, C. Chen, J. E. Haber, and R. D. Kolodner.** 1998. Genetic analysis of yeast RPA1 reveals its multiple functions in DNA metabolism. Genetics **148:**989-1005.
50. **Unsal-Kacmaz, K., A. M. Makhov, J. D. Griffith, and A. Sancar.** 2002. Preferential binding of ATR protein to UV-damaged DNA. Proc Natl Acad Sci U S A **99:**6673-6678.
51. **Wakayama, T., T. Kondo, S. Ando, K. Matsumoto, and K. Sugimoto.** 2001. Pie1, a protein interacting with Mec1, controls cell growth and checkpoint responses in Saccharomyces cerevisiae. Mol Cell Biol **21:**755-764.
52. **Zou, L., and S. J. Elledge.** 2003. Sensing DNA damage through ATRIP recognition of RPA-ssDNA complexes. Science **300:**1542-1548.
53. **Zou, L., D. Liu, and S. J. Elledge.** 2003. Replication protein A-mediated recruitment and activation of Rad17 complexes. Proc Natl Acad Sci U S A **100:**13827-13832.

**Figure Legends**

**FIG.1**. ATRIP N-terminus binds RPA70N *in vitro*.

HA-tagged, full length ATRIP or ATRIP fragments generated using a coupled transcription/translation system were incubated with (**A**) single-stranded DNA bound to sepharose beads in the presence (+) or absence (-) of purified RPA or (**B**) His-RPA bound to nickel beads. After washing, the bound proteins were eluted, separated by SDS-PAGE, blotted and probed with HA antibody. 10% of the input (In) is included for comparison. (**C** and **D**) Purified, recombinant His-tagged RPA domains were added to *in vitro* translation reactions containing HA-ATRIP, HA-ATRIPΔN (**C**) or HA-ATRIP1-107 (**D**) Protein complexes were isolated using Nickel beads, separated by SDS-PAGE, blotted and probed using an HA antibody. (**E)** Diagram of RPA heterotrimer. Black bars above protein segments indicate protein interaction domains.

**FIG.2**. A conserved acidic domain in the ATRIP N-terminus interacts with the basic cleft of RPA70N.

(**A**) The $^{15}$N-$^{1}$H-HSQC NMR spectrum of $^{15}$N-enriched-RPA70N in the absence (blue) and presence (red) of ATRIP1-107. (**B**) RPA70N residues perturbed (blue) upon addition of ATRIP1-107 mapped onto the crystal structure of RPA70N (PDB accession 2B3G). (**C**) Sequence alignment of the conserved acidic region in the N-terminus of five ATRIP orthologues. (**D**) The $^{15}$N-$^{1}$H-HSQC NMR spectrum of $^{15}$N-enriched RPA70N acquired in absence (blue) and presence (red) of ATRIP54-70. (**E**) Alignment of the p53 and ATRIP peptides used in homology modeling. (**F**) Space filling diagram of RPA70 and ATRIP55-66 (red) with the residues of RPA70N in the ATRIP binding pocket colored

blue. (**G**) Predicted electrostatic interactions between basic RPA70N basic residues K88 and R41 with ATRIP acidic residues D58 and D59.

**FIG.3**. Ddc2-Rfa1 interaction requires the conserved acidic region of Ddc2.

(**A**) Schematic diagram of ATRIP, RPA-binding mutant ATRIP (ATRIPΔN), Ddc2 and Ddc2ΔN. Location of predicted coiled-coil domains (grey) are indicated. (**B**) Δ*ddc2 HA-MEC1* yeast containing myc-vector (Vec), myc-Ddc2 (WT) or myc-Ddc2ΔN (ΔN) were exposed to 0 (-) or 60 (+) J/m$^2$ UV and harvest one hour later. Myc immunoprecipiates from soluble extracts were separated by SDS-PAGE, blotted and probed with Myc, Rfa1 and HA antibodies. (**C**) Alignment of conserved acidic region in the N-terminus of ATRIP and Ddc2 and schematic of mutations generated in this region of Ddc2. (**D**) Yeast containing TAP-Rfa1 and Ddc2 (WT), Ddc2ΔN (ΔN), Ddc2DK (DK) or Ddc2N14 (N14) were damaged with 0.01% MMS (+) or left untreated (-) and harvested one hour later. Cells were lysed and TAP-Rfa1 was isolated using IgG beads. TAP protein complexes were separated by SDS-PAGE and western blotted using Myc (Ddc2) and Rfa1 antibodies.

**FIG.4**. Ddc2 lacking the N-terminal Rfa1 binding domain is defective in localizing to sites of DNA damage.

(**A**) Δ*ddc2* yeast transformed with a centromeric plasmid expressing Myc-Ddc2 or Myc-Ddc2ΔN from the *DDC2* promoter and harboring a galactose-inducible HO endonuclease were grown to log phase in raffinose-containing media. Galactose (GAL) or glucose (GLU) was added to induce or suppress HO-endonuclease expression. One hour after

sugar addition, cells were crosslinked using formaldehyde and harvested. Cells were lysed, sonicated and Myc-Ddc2 proteins were immunoprecipitated with a myc antibody. Crosslinks were reversed and associated DNA sequences were amplified by PCR using primers specific to regions adjacent to the HO break site (HO-A, HO-B) or to the SMC2 gene (SMC2). Samples were prepared in duplicate. Input samples represent 5% of input into immunoprecipitation reactions. (**B**) Equal volumes of immunoprecipitation reactions before (pre) or after (post) isolation of Myc-Ddc2 proteins were separated by SDS-PAGE, blotted and probed with a myc antibody. (**C**) Extracts from Δ*ddc2* yeast, or yeast expressing GFP-Ddc2 (WT) or GFP-Ddc2ΔN (ΔN) were separated by SDS-PAGE and western blotted using a GFP antibody. (**D**) Yeast expressing GFP-Ddc2 (WT) or GFP-Ddc2ΔN (ΔN) and galactose-inducible HO-endonuclease were grown to log phase in liquid culture. Glucose (GLU) or galactose (GAL) were added to suppress or induce DNA double strand break formation. GFP fluorescence was visualized on a Zeiss Axioplan fluorescent microscope. (**E**) Quantitation of HO-induced focus formation of GFP-Ddc2 or GFP-Ddc2ΔN 4 hr or 6 hr after induction of HO endonuclease expression. Error bars represent standard deviation from three experiments.

**FIG.5**. Disruption of Ddc2-Rfa1 interaction impairs the DNA damage response.

(**A** and **B**) Yeast lacking Ddc2 (vector), or expressing Ddc2 (WT), Ddc2ΔN (ΔN), Ddc2DK (DK) or Ddc2N14 (N14) were grown to log phase in liquid culture and plated onto rich media containing increasing amounts of (**A**) HU or (**B**) MMS. Percent viability was calculated as the number of colonies surviving at each dose compared to the number of colonies that survived on plates lacking HU or MMS. Data represent the average of

three experiments. Standard deviations were smaller than symbol width in most cases. (**C-E**) Yeast strains were arrested in G1 with alpha factor and released into rich media in the presence if 200 mM HU (**C** and **E**) or in the indicated concentration of HU (**D**). Cells were harvested one hour (**C** and **D**) or at the indicated times (**E**) after G1 release and TCA precipitated. Lysates were separated by SDS-PAGE, blotted and probed with Rad53 or Myc antibodies. (**F** and **G**) Δ*ddc2* (V), *DDC2* (WT) or *ddc2ΔN* (ΔN) yeast were grown to log phase in liquid culture, arrested in G1 with alpha factor and released into media containing the indicated doses of MMS and harvested one hour post G1 release (**F**) or at the indicated various time points after G1 release (**G**). Cells were lysed, proteins were separated by SDS-PAGE, blotted and probed with Rad53 antibody. (**G**) Membranes containing immobilized proteins were subjected to in-situ autophosphorylation to assay Rad53 autophosphorylation activity.

**FIG.6**. TopBP1 activates ATR-ATRIP complexes independently of RPA.

(**A**) Wild-type ATR-ATRIP or ATR-ATRIPΔN complexes were isolated from transfected 293T cells and incubated with recombinant wild-type TopBP1 978-1286 (WT) or TopBP1 978-1286 W1145R (WR), Phas1 substrate, and γ-$^{32}$P-ATP. Kinase reactions were separated by SDS-PAGE, stained with coomassie and exposed to film ($^{32}$P). A duplicate gel was blotted and probed with anti-ATRIP and anti-ATR antibodies (WB). (**B**) Wild-type ATR-ATRIP or kinase-dead ATR-ATRIP immune complexes were isolated from transfected 293T cells and incubated with recombinant TopBP1 and/or RPA heterotrimer in the presence of Phas1 substrate and γ-$^{32}$P-ATP. Kinase reactions were separated by SDS-PAGE, stained with coomassie or blotted, and exposed to film

($^{32}$P) or probed with anti-ATR antibodies (WB). (**C** and **D**) 293T cells stably expressing siRNA-resistant ATRIP, ATRIPΔN, or empty vector control were transfected with ATRIP siRNA to deplete endogenous ATRIP. Two days after siRNA transfection, the cells were transfected with GFP-TopB1 978-1286 expression construct. Twenty-four hours later the cells were fixed and stained with antibodies to γH2AX. (**C**) Representative images collected on a Zeiss Axioplan microscope with the same exposure times. (**D**) Quantitation of the percentage of the GFP-TopBP1 expressing cells that contained phosphorylated H2AX. Error bars represent the standard deviation. The inset is a western blot showing the relative expression levels of ATRIP and ATRIPΔN.

| Strain | Description/genotype | Reference |
|---|---|---|
| DMP2995/1B | *MAT* **a** *ade2-1 can1-100 his3-11,15 leu2-3,112 trp1-1 ura3 sml1 ::KanMX4* | Paciotti *et. al.(2000)* |
| yHB200 | DMP2995/1B [p1220: *Myc-URA3-CEN* ] | This study |
| yHB201 | DMP2995/1B [pNML1: *Myc-DDC2-URA3-CEN* ] | This study |
| yHB202 | DMP2995/1B [pHB126: *Myc-ddc2ΔN-URA3-CEN* ] | This study |
| yHB221 | DMP2995/1B [pHB157: *Myc-ddc2D12KD13K-URA3-CEN* ] | This study |
| yHB222 | DMP2995/1B [pHB155: *Myc-ddc2NAAIRS14-19-URA3-CEN* ] | This study |
| Rfa1-TAP | *MAT* **a** *his3-1 leu2-0 met15-0 ura3-0 Rfa1-TAP* | Ghaemmaghami *et. al.(2003)* |
| yHB231 | Rfa1-TAP [pNML1: *Myc-DDC2-URA-CEN* ] | This study |
| yHB232 | Rfa1-TAP [pHB126: *Myc-ddc2ΔN-URA-CEN* ] | This study |
| yHB233 | Rfa1-TAP [pHB157: *Myc-ddc2D12KD13K-URA3-CEN* ] | This study |
| yHB234 | Rfa1-TAP [pHB155: *Myc-ddc2NAAIRS14-19-URA3-CEN* ] | This study |
| JKM179 | *hoΔ MAT* **a** *hmlΔ::ADE1 hmrΔ::ADE1 ade1-100 leu2-3,112 lys5 trp1::hisG' ura3-52 ade3::GAL::HO* | Lee *et. al. (2003)* |
| yHB244 | JKM179 *ddc2Δ::URA3* [pBAD79: *RNR3-TRP1-CEN* ] | This study |
| yHB245 | yHB244 (GAL-HO, Δ*ddc2* ) [p1220: *Myc-URA3-CEN* ] | This study |
| yHB246 | yHB244 (GAL-HO, Δ*ddc2* ) [pNML1: *Myc-DDC2-URA3-CEN* ] | This study |
| yHB247 | yHB244 (GAL-HO, Δ*ddc2* ) [pHB126: (*Myc-ddc2ΔN-URA3-CEN* ] | This study |
| yJK8-1 | *Mat Δ, can1 ade2 trp1 his3 ura3 leu2 lys5 cyh2 ade3::GalHO adh4::HO site::HIS3 DDC2-GFP::KanR* | Melo *et. al.(2001)* |
| yHB255 | yJK8-1 *GFP-ddc2ΔN* [pBAD79: *RNR3-TRP1-CEN* ] | This study |

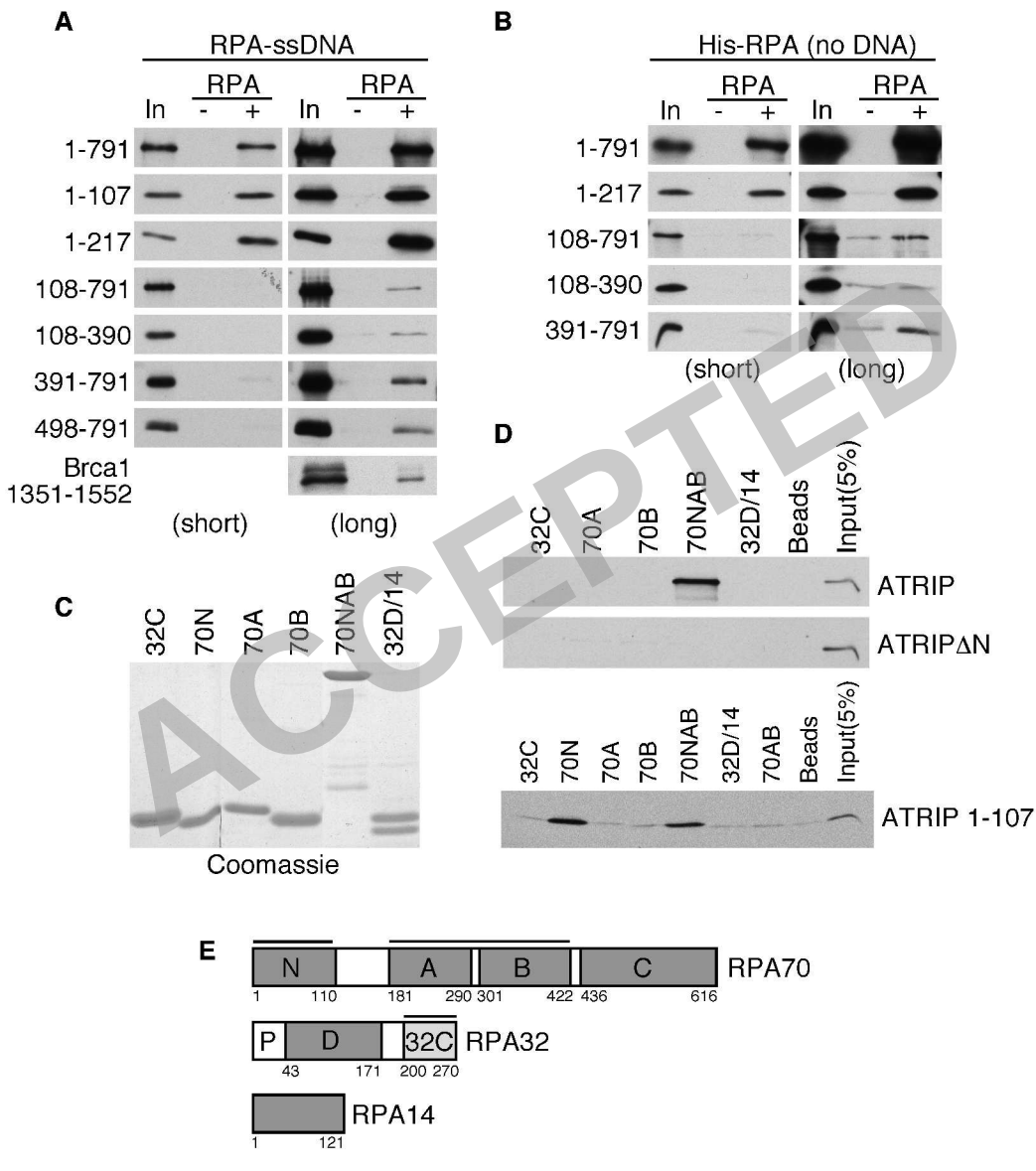




**Figure 1**

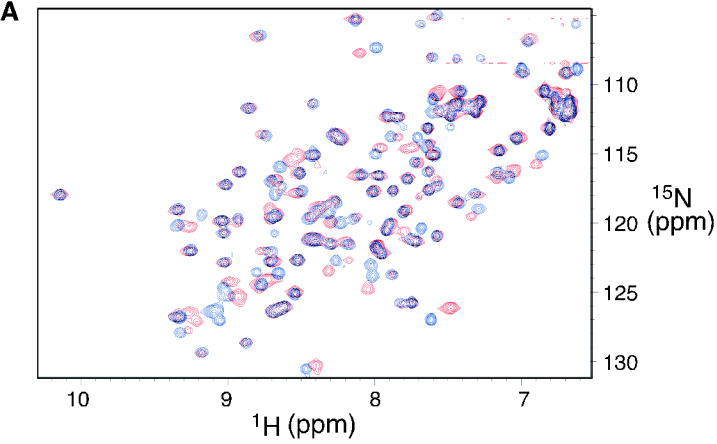


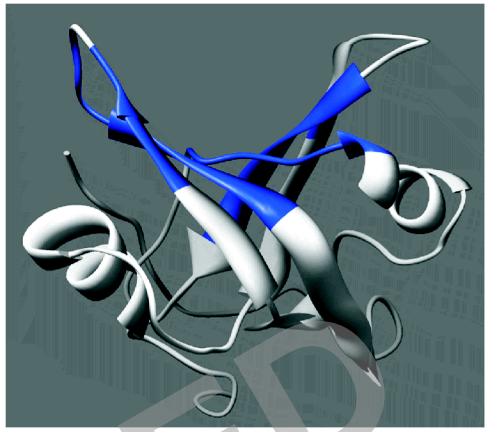


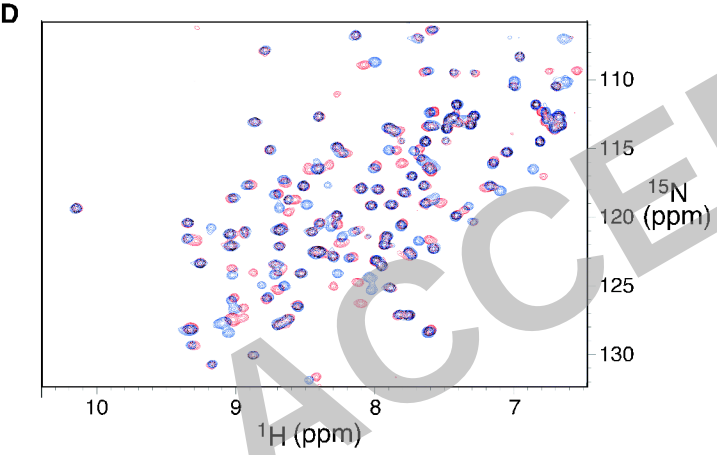




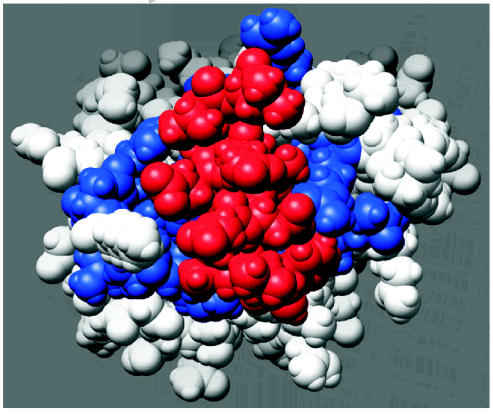


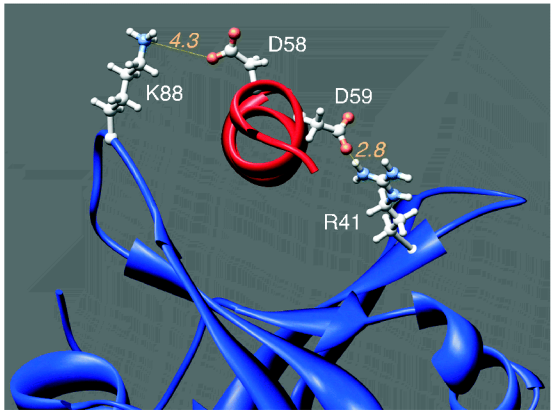




**Figure 2**

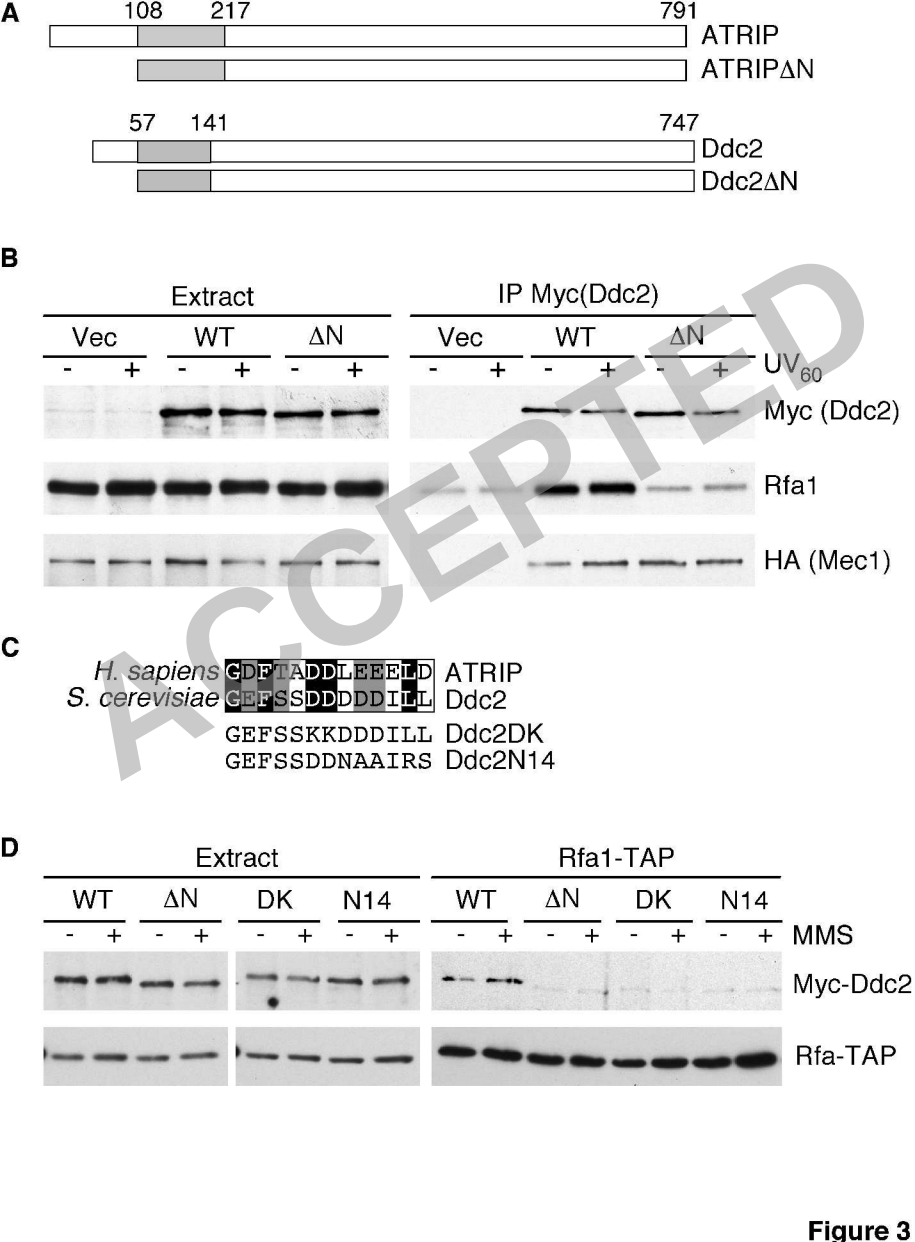




**Figure 3**

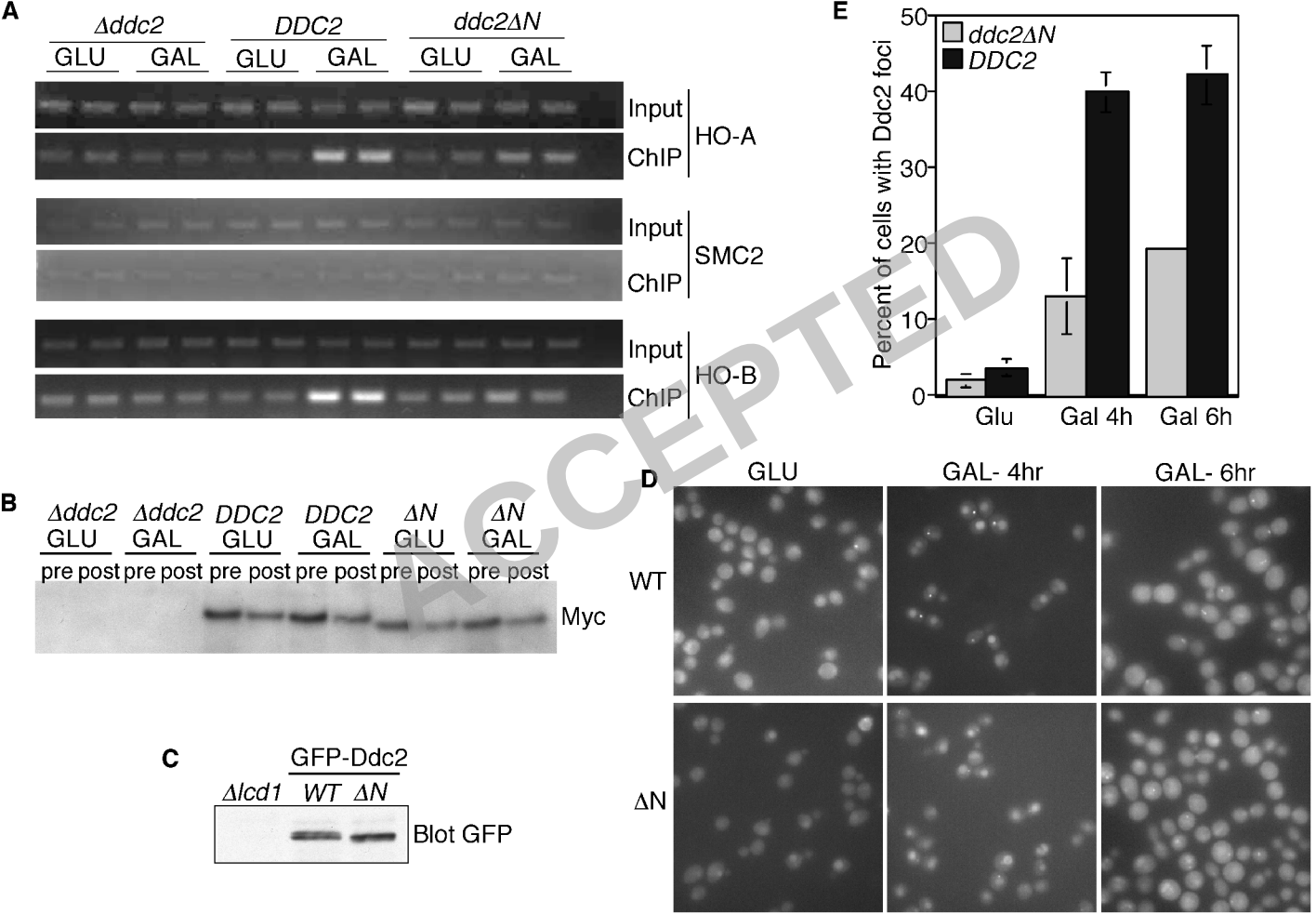




**Figure 4**

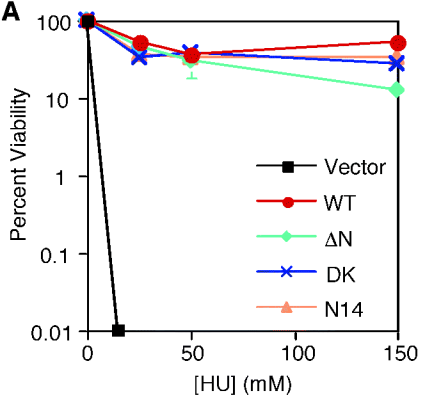


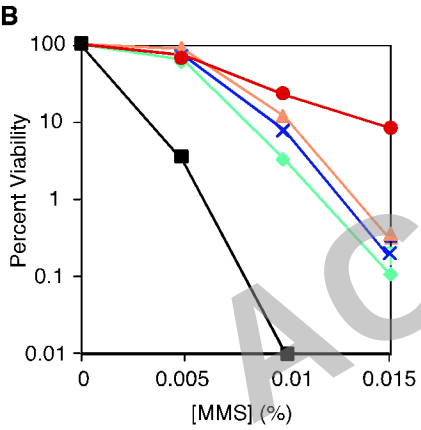


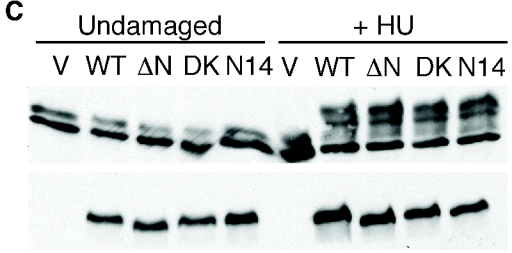


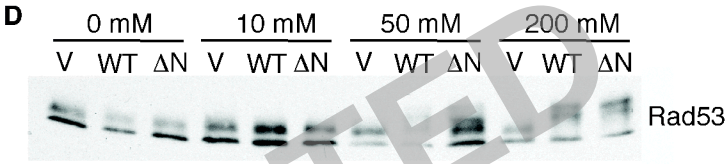


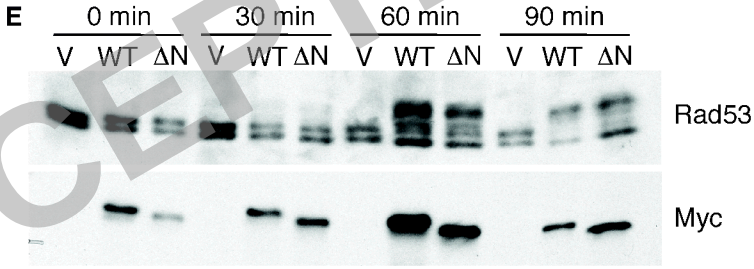


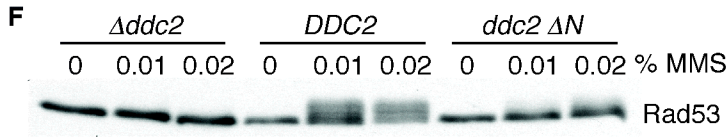


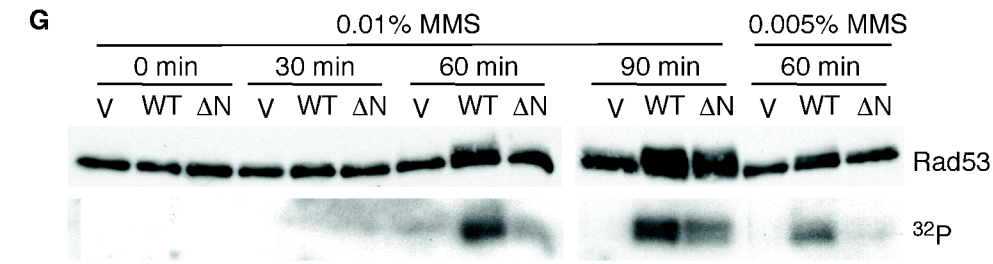




**Figure 5**

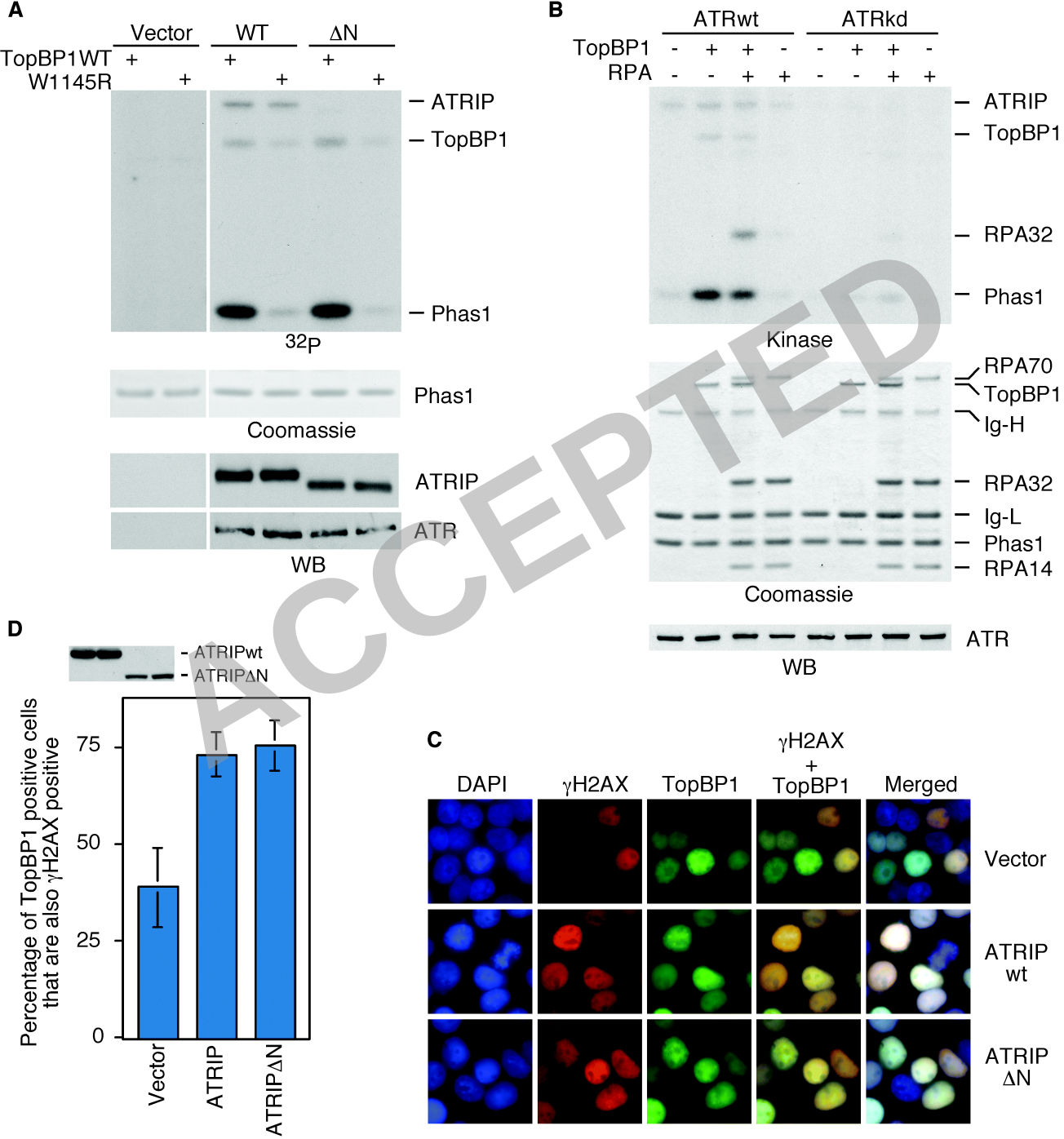




**Figure 6**